

# FDFD Inverse Design Acceleration of $3 \times 3$ Hub Device Based on the Schur Complement Domain Decomposition Method

Jin Li

1 Tsinghua Shenzhen  
International Graduate  
School

Tsinghua University  
Shenzhen, China

2 Peng Cheng Laboratory  
Shenzhen, China  
lijin22@mails.tsinghua.edu.cn

Houyu Chen

Tsinghua Shenzhen  
International Graduate  
School

Tsinghua University  
Shenzhen, China

chenhouy21@mails.tsinghua.edu.cn

Lirong Cheng

Tsinghua Shenzhen  
International Graduate  
School

Tsinghua University  
Shenzhen, China

clr18@mails.tsinghua.edu.cn

Zhenmin Chen

Peng Cheng Laboratory  
Shenzhen, China  
chenzhm@pcl.ac.cn

Zhengdong Liu

Peng Cheng Laboratory  
Shenzhen, China  
liuzht02@pcl.ac.cn

Connie Chang-Hasnain

Tsinghua Shenzhen  
International Graduate  
School

Tsinghua University  
Shenzhen, China  
cch@sz.tsinghua.edu.cn

H. Y. Fu

Tsinghua Shenzhen  
International Graduate  
School

Tsinghua University  
Shenzhen, China  
hyfu@sz.tsinghua.edu.cn

**Abstract**—We realized the inverse design of  $3 \times 3$  hub device through Schur complement domain decomposition method, reducing the size of FDFD solution matrix by dividing the area of devices, which realized 2.95 times the acceleration ratio.

**Keywords**—Schur complement domain decomposition, inverse design, electromagnetic field simulation acceleration, FDFD solution

## I. INTRODUCTION

Micro and nanophotonic devices play an important role in optical communication, high-performance computing, optical information processing, optical interconnect and other fields [1]. The inverse design method has achieved remarkable results in the design of high-performance optical devices [2]. In the process of inverse design, the optimization time increases significantly as the design area gets larger. Therefore, improving the computational efficiency of photonic structures has become a hot research field.

In photonic design, the acceleration based on domain decomposition technology has had many successful applications, among which the Schur complement domain decomposition is an effective method [3], and as a domain decomposition method (DDM) [4-7] it is usually used to accelerate computations. For the inverse design of micro and nanophotonic devices, the device structure that needs to be designed usually only occupies a part of the entire computing area [8,9]. Thus, the computing scale will greatly increase as the device size gets larger. In each step of the design optimization, if only the design area is calculated, the calculation amount will be greatly reduced and the efficiency will be improved. In the finite difference frequency domain (FDFD) simulation calculation, the calculation amount is mainly determined by the dimension of sparse matrix and the number of non-zero elements in its matrix. Therefore, dividing the calculation area and design area based on the Schur complement domain decomposition method can effectively reduce the size of the solution matrix.

The Schur complement domain decomposition method in this study realized the inverse design of micro and nanophotonic devices, significantly improved the computational efficiency, and successfully designed  $3 \times 3$  hub, achieving an acceleration ratio of 2.95 times in the preconditioning system. This explains the applicable scale and acceleration efficiency of the Schur complement domain decomposition preconditioning system in 1D, 2D and 3D. It provides a possibility for the large-scale design of micro and nanophotonic devices and the design of devices with complex functions.

## II. THEORY OF THE SCHUR COMPLEMENT DOMAIN DECOMPOSITION METHOD

In this section, we discuss the theory of Schur complement domain decomposition method. First, we provide the Schur complement decomposition applied to the Maxwell's equations in FDFD. The Maxwell equation for the E-field is

$$\left( \frac{1}{\mu_0} \nabla \times \nabla \times - \omega^2 \epsilon_0 \epsilon_r(r) \right) \mathbf{E}(r) = -i\omega \mathbf{J}(r). \quad (1)$$

The equation above can be discretized by the finite difference method on the Yee mesh, which can be converted into a system of linear equations as

$$A\mathbf{E} = -i\omega \mathbf{J}, \quad (2)$$

where  $A$  represents the discrete approximation on the left side of the equation.  $\mathbf{E}$  in the above equation is now a vector, including the unknown amount of mesh nodes in each space, and  $\mathbf{J}$  is also a vector, containing the source information on these discrete domains. Now we consider decomposing the design area in the optical simulation device. The design area is represented by the subscript  $O$ , which is the area for optimization. The background area is represented by the subscript  $B$ , which includes the rest of the calculation area. In this case, the background includes a perfectly matched layer (PML) together with left and right waveguides (input and

output sources). By sorting out the above formula, it can be expressed in a  $2 \times 2$  matrix form as

$$\begin{bmatrix} A_O & A_{OB} \\ A_{BO} & A_B \end{bmatrix} \begin{bmatrix} E_O \\ E_B \end{bmatrix} = -i\omega \begin{bmatrix} J_O \\ J_B \end{bmatrix}. \quad (3)$$

The submatrices  $A_O$  and  $A_B$  are discrete representations of the above equations, which are respectively limited to the design area and background area. The  $A_{OB}$  and  $A_{BO}$  on the diagonal represent the spatial coupling of the mesh nodes on the interface of the two areas, and the coupling happens in the interface of the background area and design area, thus we can get the second row of the above equation

$$A_{BO}E_O + A_BE_B = -i\omega J_B. \quad (4)$$

We can solve  $E_B$  and substitute it into the first row of the equation to obtain  $E_O$ ,

$$SE_O = -i\omega J_S \quad (5)$$

Thus

$$S \equiv A_O - A_{OB}A_B^{-1}A_{BO} \quad (6)$$

$$J_S \equiv J_O - A_{OB}A_B^{-1}J_B. \quad (7)$$

Finally, we can get

$$E_B = A_B^{-1}(J_B - A_{BO}E_O). \quad (8)$$

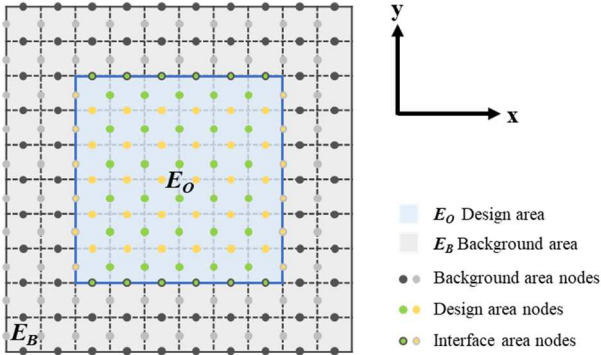


Fig. 1. Schematic diagram of Schur complement domain decomposition Yee mesh division.

In the design of micro and nanophotonic devices, for a given structure, only a part of the structure needs to be optimized, while the rest of the structure remains unchanged through the inverse design method. As shown in Fig. 1, the design optimization area usually only occupies a small part of the entire calculation area. For the process of the solution optimization through the electromagnetic field simulation algorithm, in each iteration step of optimization, although the gray background area remains unchanged during the iteration, the entire device structure area still needs to be simulated and optimized.

Equation (3) shows the original system of electromagnetic field numerical calculation in the process of inverse design, while equation (5) is for the system after the preconditioning process through Schur complement decomposition. Because of the nodes coupling on the interface of the background area

and the design area,  $A_{OB}$  is a non-zero matrix, after the process of Schur complement preconditioning, the field source information  $J_B$  outside the design area in the original system now can be represented by the filed source  $J_S$  of the background area which contains only the information in the design area. The simplified system contains only the design area  $E_O$ . To form an equivalent original system  $E$ , it only needs to calculate  $A_{OB}A_B^{-1}A_{BO}$  and  $A_{OB}A_B^{-1}J_B$ , which is the Schur matrix, and it can be calculated directly or by the iterative solver. And this process only needs to be calculated once in the whole inverse design electromagnetic field numerical calculation process, so it can effectively reduce the calculation scale, reducing the calculation time.

### III. THE INVERSE DESIGN OF $3 \times 3$ HUB DEVICE

Based on the above Schur complement domain decomposition preconditioning algorithm, we have built an inverse design platform. In the specific device design, as demonstrated in Fig. 2, the 2D diagram of the  $3 \times 3$  hub, the area in light yellow exhibits the input and output ports, the light source enters from the left side and outputs on the right side, the area in light blue is the area where the calculation needs to be optimized, and the area in gray is the residual structure part. In this way, the matrix scale to be optimized in each iteration step is effectively reduced through Schur complement preconditioning, so as to improve the calculation efficiency.

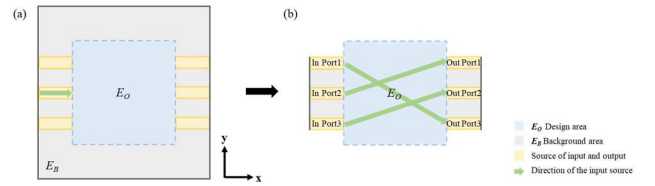


Fig. 2. 2D diagram of  $3 \times 3$  hub (a) device simulation area in the original system, (b) device simulation area after simplified by Schur complement decomposition preconditioning system.

We designed the  $3 \times 3$  hub on the area shown in Fig. 3. It realized the  $3 \times 3$  multi-port forwarding function at wavelength  $\lambda = 1.55 \mu\text{m}$ , and the paths of the left-to-right incident light are: In Port1  $\rightarrow$  Out Port3, In Port2  $\rightarrow$  Out Port1, In Port3  $\rightarrow$  Out Port2. Then the investigation was carried out. Fig. 2 shows the benchmark structure of the device being simulated, and the amount of mesh in its calculation area is  $120 \times 120$ , accounting for  $4.8 \mu\text{m} \times 4.8 \mu\text{m}$ . Each mesh size is set to  $40 \text{ nm} \times 40 \text{ nm}$ . The area relevant with Schur complement domain decomposition method also includes the input and output source of  $3 \times 3$  hub. In the optimization process, we assumed that the initial structure of the design area is uniform, and the relative dielectric permittivity is 2.25.

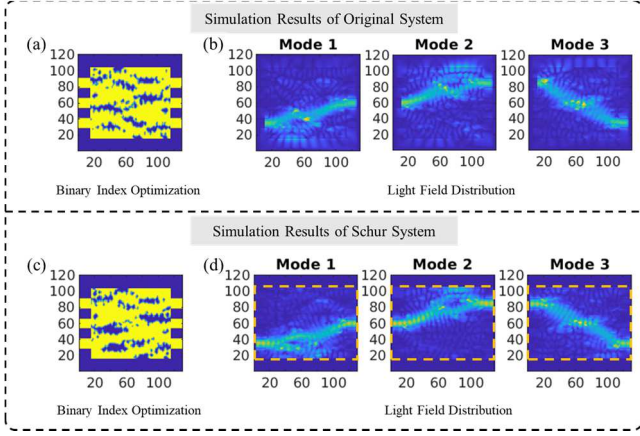


Fig. 3.  $3 \times 3$  hub device (a) diagram of original system device simulation structure (b) diagram of original system light field distribution, (c) diagram of Schur complement domain decomposition system device simulation structure, (d) diagram of Schur complement domain decomposition system light field distribution.

In the two-dimension simulation of  $3 \times 3$  hub, it can be observed from Fig. 2 that its design area in yellow accounts for only  $3.6 \mu\text{m} \times 3.6 \mu\text{m}$  in the total calculation area. Therefore, the Schur complement preconditioning method has a good advantage. The background area located at the upper and lower boundaries does not participate in the electromagnetic field numerical calculation of each iteration, which makes the single-step time of electromagnetic field simulation significantly reduced in each calculation, thus improving the overall calculation efficiency.

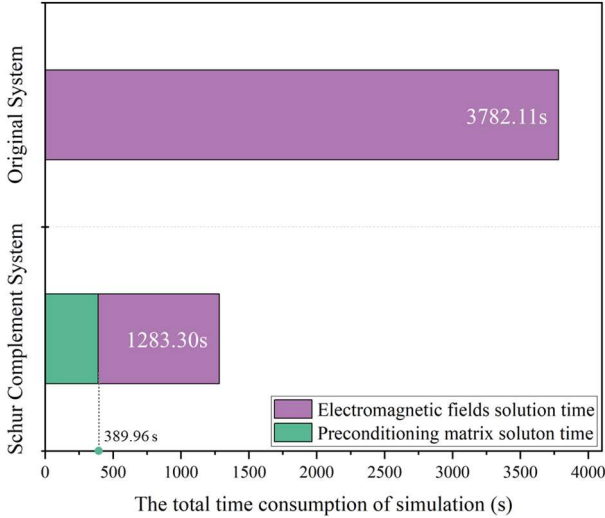


Fig. 4. The diagram of  $3 \times 3$  hub simulation total time consumption in Schur complement domain decomposition preconditioning system and original system.

According to the numerical calculation results of the electromagnetic field, the total time of Schur complement preconditioning algorithm comes from two aspects. On the one hand, it contains the time to calculate Schur matrix in the preconditioning process, and on the other hand it contains the time of the electromagnetic field numerical calculation. As illustrated in Fig. 4, the time to calculate Schur matrix is 389.96 s, and the time spent in electromagnetic field numerical calculation after preconditioning will be significantly reduced, only 893.37 s. Then the total time consumption based on Schur complement preconditioning algorithm is 1283.3 s, and

the simulation time of the original system is 3782.11 s. In the numerical calculation of electromagnetic field, the average single-step calculation time of the system after Schur complement preconditioning is 4.30 s, and the average single-step calculation time of the original system is 49.12 s. This shows that the matrix scale of its electromagnetic field numerical calculation can be effectively reduced through Schur complement preconditioning. This algorithm achieved 2.95 times the acceleration ratio for the total calculation time and significantly reduced the single-step simulation time, thus improving the overall simulation efficiency.

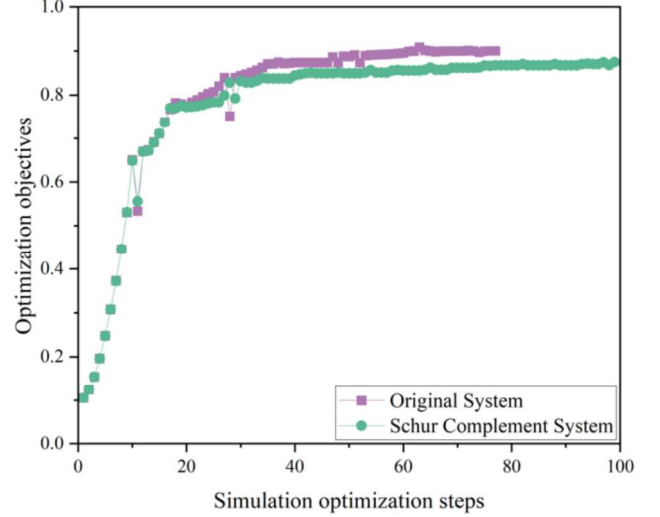


Fig. 5. The optimization objectives diagram of  $3 \times 3$  hub Schur complement domain decomposition preconditioning system and original system.

The simulation environment with the combination of FDFD and Python is applied to carry out the inverse design for the device with adjoint optimization and level-set approach, and after 100 iterations, according to Fig. 5, we can see that the optimization accuracy rate based on Schur complement preconditioning algorithm can be consistent with that of the original system, which verifies the deduction conclusion in section II. By effectively dividing the background area and design area, we only need to solve the Schur matrix once. The simplified system only includes the design area  $E_0$ , and the equivalent original system  $E$  can be obtained through equations (6) and (7).

#### IV. SUITABLE RANGE OF SCHUR COMPLEMENT PRECONDITIONING METHOD

With the increase of the size and complexity of the device simulation matrix, the total time consumption of the Schur complement preconditioning method has increased. Therefore, we further explored the quantitative relationship between the number of Yee mesh nodes and the non-zero elements of the sparse matrix, and explored the applicable scale of its Schur complement preconditioning method. In FDFD simulation calculation, the calculation amount is mainly determined by the dimension of sparse matrix and the number of non-zero elements in its matrix. As demonstrated in Fig. 6, we assume that our background area and design area are square, the gray area is the device calculation area, and the area in light blue is the device design area.  $N$  refers to the number of mesh points per side of the background area and  $n$  represents the number of mesh points per side of the design area. The arrow indicates the location of the source, and shows the contribution to the sparse mode of the original calculation area matrix after using

Schur complement decomposition in 1D, 2D, and 3D. Its contribution mainly comes from two aspects, elements on Schur complement domain decomposition interface and elements inside the design area.

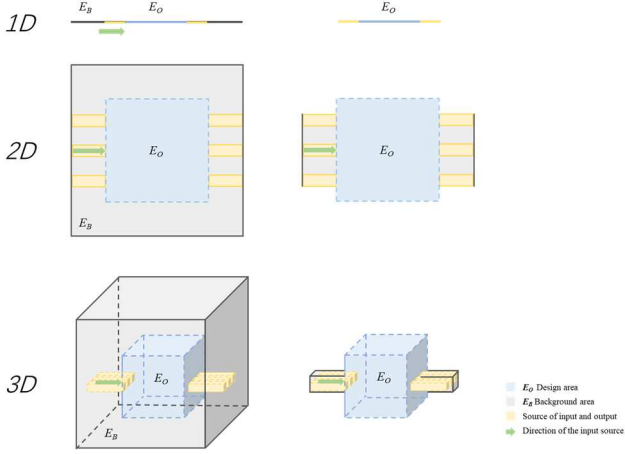


Fig. 6. Diagram of inverse design of photonic devices in 1D, 2D and 3D

From this, we can deduce the contribution of Schur complement domain decomposition to the original calculation area matrix sparse mode in 1D, 2D and 3D.  $A$  is noted as the non-zero matrix elements of the original system, and  $S$  is the number of non-zero elements that the Schur complement system contributes to its sparsity. The acceleration effect reaches the best when  $S = A$ .

In the case of 1D,  $A$  refers to non-zero matrix element  $3N(N_x)$ ,  $S$  refers to two contributions to its sparsity, one part is  $2n - 2$  on the interface, and the other is  $3(n - 2)$  inside the design area, the number of non-zero elements contributed together is  $(2n - 2) + 3(n - 2)$ , when  $S = A$ ,  $n/N \approx 0.6$  is obtained.

In the case of 2D,  $A$  refers to non-zero matrix element  $5N^2(N_x N_y)$ ,  $S$  refers to two contributions to its sparsity, one part is  $(4n - 2)^2$  on the interface, and the other is  $5(n - 2)^2$  inside the design area, the number of non-zero elements contributed is  $(4n - 2)^2 + 5(n - 2)^2$ , when  $S = A$ ,  $n/N \approx 0.5$  is obtained [9].

In the case of 3D,  $A$  refers to non-zero matrix element  $13N^3(N_x N_y N_z)$ ,  $N = 3n_x n_y n_z$ ,  $S$  refers to two contributions to its sparsity, one part is  $(12n - 2)^3$  on the interface, and the other is  $13(n - 2)^3$  inside the design area, and the number of non-zero elements contributed in total is  $(12n - 2)^3 + 13(n - 2)^3$ . When  $S = A$ ,  $n/N \approx 0.2$  is obtained, so the acceleration effect in 3D is not significant.

TABLE I. QUANTITATIVE RELATIONSHIP BETWEEN THE NUMBER OF MESH NODES AND NON-ZERO ELEMENTS OF SPARSE MATRIX

Dimension	A: Non-zero matrix elements	Contribution on the interface	Contribution inside the design area	S: Total non-zero elements contributed	$n/N$
1D	$3N(N_x)$	$2n - 2$	$3(n - 2)$	$(2n - 2) + 3(n - 2)$	0.6
2D	$5N^2(N_x N_y)$	$(4n - 2)^2$	$5(n - 2)^2$	$(4n - 2)^2 + 5(n - 2)^2$	0.5

3D	$13N^3(N_x N_y N_z)$	$(12n - 2)^3$	$13(n - 2)^3$	$(12n - 2)^3 + 13(n - 2)^3$	0.2
----	----------------------	---------------	---------------	-----------------------------	-----

Therefore, in the future, we can use the combination of the adaptive mesh algorithm [10] and Schur complement preconditioning algorithm to represent the design area and background area of the device with different spatial resolutions to further reduce the size of the calculation matrix, effectively solve the limitation of the application range of single Schur complement preconditioning method, and significantly improve the speed of large-scale 3D device design.

## V. CONCLUSION

We designed a  $3 \times 3$  hub, realized an acceleration ratio of 2.95 times in the acceleration scheme based on Schur complement domain decomposition system, and it maintained good accuracy. At the same time, it demonstrates the suitable range of the Schur complement domain decomposition algorithm in 1D, 2D and 3D. This method provides an efficient scheme for the design of larger-scale micro and nanophotonic devices. In the future, the storage cost of Schur complement matrix can be reduced by finding its sparse approximate solutions, so as to further improve the calculation efficiency and broaden its suitable range.

## ACKNOWLEDGMENT

The authors would like to express sincere thanks to the Shenzhen Fundamental Research Program (No. GXWD20201231165807007202008-27130534001) and the Major Key Project of PCL.

## REFERENCES

- [1] Atabaki A H, Moazeni S, Pavanetto F, et al, "Integrating photonics with silicon nanoelectronics for the next generation of systems on a chip" Nature vol. 556.7701, pp. 349-354, 2018.
- [2] Molesky, S., Lin, Z., Piggott, A.Y. et al, "Inverse design in nanophotonics". Nature Photon vol. 12.11, pp. 659-670, 2018.
- [3] Zhao N, Verweij S, Shin W, Fan S, "Accelerating convergence of an iterative solution of finite difference frequency domain problems via schur complement domain decomposition". Optics Express vol. 26.13, pp. 16925-16939, 2018.
- [4] L. Kulas and M. Mrozowski, "Low-reflection subgridding" IEEE Trans. Microwave Theory Tech. vol. 53.5, pp. 1587-1592, 2005.
- [5] J. Podwalski, P. Kowalczyk, and M. Mrozowski, "Efficient multiscale finite difference frequency domain analysis using multiple macromodels with compressed boundaries" Progress In Electromagnetics Research. vol. 126, pp. 463-479, 2012.
- [6] G. Fotyga, P. Kowalczyk, L. Kulas, K. Nyka, J. Podwalski, and M. Mrozowski, "Reduced order models in computational electromagnetics (in memory of Ruediger Vahldieck)" 2012 Asia-Pacific Symposium on Electromagnetic Compatibility, pp. 705-708, 2012.
- [7] H. Luan, Y. Geng, Y. Yu, and S. Guan, "Three-dimensional transient electromagnetic numerical simulation using FDFD based on octree grids" IEEE Access vol. 7, pp. 161052-161063, 2019.
- [8] Jaysaval P, Shantsev D, de la Kethulle de Ryhove S, "Fast multimodel finite-difference controlled-source electromagnetic simulations based on a Schur complement approach". Geophysics, vol. 79.6, pp. E315-E327, 2014.
- [9] N Zhao, S. Boutami, and S. Fan, "Accelerating Adjoint Variable Method Based Photonic Optimization with Schur Complement Domain Decomposition" Optics Express vol. 27.15, pp. 20711-20719, 2019.
- [10] Wang Q, Liu H, Cui X, et al, "Acceleration of inverse design process on adaptive mesh" Optics Express, vol. 29.16, pp. 25064-25083, 2021.